PHYSICAL REVIEW B VOLUME 55, NUMBER 20 15 MAY 1997-II

Local structural and vibrational properties of stepped surfaces: Cu(211), Cu(511), and Cu(331)

Sondan Durukanoğlu, Abdelkader Kara, and Talat S. Rahman
Department of Physics, Cardwell Hall, Kansas State University, Manhattan, Kansas 66506

(Received 23 December 1996)

We present a comparative study of the local structural and vibrational properties of three regularly stepped surfaces of Cu which have similar terrace widths. The local vibrational density of states are evaluated using a real-space method with the force-constant matrix generated from a many-body, semiempirical potential based on the embedded-atom method. We find that the multilayer relaxation pattern for Cu(331) is quite different from Cu(211) and Cu(511). Furthermore, we show that the relaxations of the step atoms are dictated by the lower coordinations of their surrounding atoms. Our calculations also show that the local vibrational properties of the three vicinal surfaces of Cu are sensitive to their local atomic environment. [S0163-1829(97)01720-7]

I. INTRODUCTION

The morphology of surfaces at an atomic level plays a crucial role in determining the behavior of surfaces in many physical phenomena, including epitaxial growth, chemical reactivity, and the stability of crystals.[1] On any real surface, steps are unpreventably present, and their nature describes the morphology of surfaces. These surface defects are expected to serve as nucleation regions and to affect the energetics, reactivity, and dynamic properties of the surface because of the unsaturated coordination sites in their vicinity.[2] Key questions concerning the behavior of the surface in the processes mentioned above are closely related to the rearrangment of electronic and ionic structure induced by the presence of these surface defects. Due to Smoluchowski charge smoothing of the electron charge density around a step,[3] electrons are expected to move from the step edge toward the lower terrace, yielding a local rearrangement of electronic and ionic structures. As a consequence of this charge redistribution, the force fields in the region of these surface defects may be modified, resulting in local structural relaxation of atoms around steps, in addition to the relaxation of the whole surface layer. Thus studies of the structural relaxations around the local environment of defects can be informative about defect induced-charge redistribution. The modification of the local force fields also alters the vibrational properties of the surface, as manifested in the characteristics of localized modes around these surface defects. In the case of stepped surfaces in particular, the existence of stepped localized modes[4] and the ''backfolding'' of the modes, due to the reduction of the surface Brillouin zone,[6–8] are expected. These vibrational characteristics can be used to analyze the force fields in the vicinity of steps. The studies of vibrational dynamics can also lead to an evaluation of the thermodynamic properties which control the stability of steps.

With advances in atomic scale experimental and theoretical techniques, there has been a surge in studies, in recent years, related to the structural and vibrational properties of high Miller index, or vicinal, surfaces. Except for a few first-principles electronic structure calculations,[9,10] most of the theoretical investigations of the surface structure of vicinal surfaces have been based on simple model potentials. The experimental methods for structural determination have usually involved low-energy electron diffraction (LEED) (Ref. 11) or low-energy ion scattering.[12] Although these surface structure studies have focused on different types of stepped surfaces of various fcc metals, a few general trends have been found. For example, for Al(331),[9,11] Al(211),[13] Al(511),[14] and all fcc(211),[15] the relaxation of the interlayer spacings shows an oscillatory behavior of (-,-,+,-,-,+,-,…) with decreasing magnitude away from the surface into the bulk. For Cu(410),[12] Al(331),[9] and Pt(775) (Ref. 5) step atoms display a slight inward relaxation toward the remainder of the metal, supporting the view of a charge smoothing effect around steps. As for the vibrational properties of stepped surfaces, since the pioneering work of Ibach and Bruchman on Pt(775) using the inelastic electron scattering technique,[4] detailed analyses of Al(221),[16] Ni(977),[17] and Cu(211) and Cu(511) (Ref. 18) have been performed with the inelastic He-surface scattering method. On the theoretical side, several studies of high Miller-index surface vibrational modes have been reported.[5–7,19–24] The earlier measurements by Ibach and Bruchmann[4] showed the existence of a high-frequency vibrational mode associated with the step of Pt(755). This mode was further identified in a theoretical study based on the tight-binding model by Allan as induced by step relaxations.[5] The high frequency of the Pt(775) mode was ascribed to the stiffening of the force constants at the surface as compared to that in the bulk metal. More recently on Ni(977), Niu *et al.*[17] found a low-frequency mode which they attributed to a softening of the force constants in the vicinity of the step. Similar He-atom scattering measurements by Witte *et al.* for the Cu(211) surface[18] also exhibit a low-frequency surface mode whose origin is proposed to lie in the relaxations at and near the step. This set of experimental data on step-localized modes point to the changes in the force fields at and near steps, and to their implications for the characteristics of these modes.

In this work, it is our aim to investigate the structural and vibrational properties of some vicinal, or regularly stepped, surfaces of Cu. Our main interest here is in a comparative study of three types of surfaces, namely, (331), (211), and (511). These are chosen because they have similar terrace widths, and possess different surface geometry, thereby allowing an examination of the influence of the local

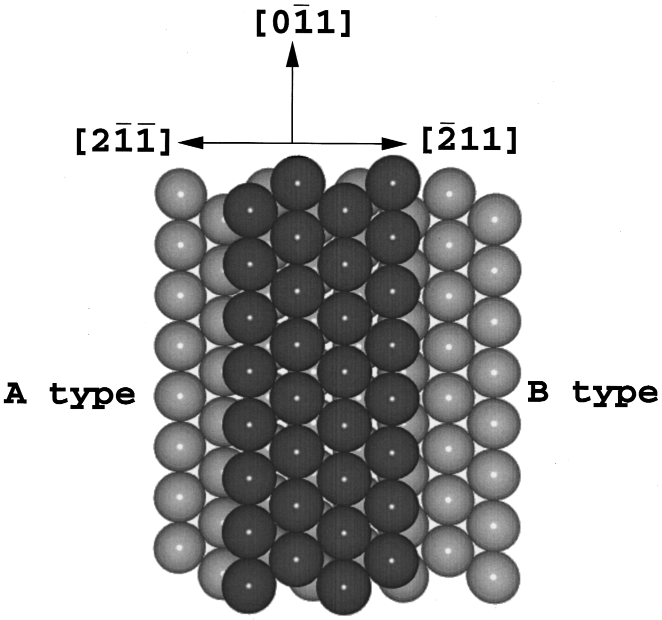

FIG. 1. Top view of a fcc(111) surface. The [111] direction is pointing out of the page. Cutting the crystal toward [211] creates *B*-type steps, whereas cutting the crystal toward [211] creates *A*-type steps.

atomic structure on its characteristics. We are also motivated by the availability of He-atom scattering data for the phonons on two of these systems. Among the issues investigated here are the multilayer relaxation patterns of these three different types of stepped surfaces, local relaxations, and force-constant modifications around the step atoms. The frequencies and polarizations of the surface modes and the characteristics of the local density of states and the thermodynamic functions of step atoms are also examined.

The rest of this report is organized as follows. Section II contains a brief summary of the geometry of the stepped surfaces studied here, while the theoretical methods for obtaining the force-constant matrix and the local vibrational density of states are presented in Sec. III. Our results and discussions are summarized in Sec. IV.

II. GEOMETRY

Vicinal surfaces can easily be constructed by cutting the crystal at an angle slightly off from the lower-index crystal planes [i.e., (100), (111), and (110) planes]. We are interested here in the vicinals of the fcc(100) and fcc(111) surfaces, of which the most tightly packed steps are along the [110] direction. Since on the fcc(111) surface the [110] direction is not parallel to any plane of symmetry, there exist two different ways of generating monoatomic stepped surfaces (see Fig. 1). Thus the vicinals of the fcc(111) surfaces are classified as fcc$(n,n,n\pm 2)$, while the vicinals of the (100) are labeled fcc$(2n-1,1,1)$, if only monoatomic steps and unkinked step edges are considered.[16] The first class of surfaces is composed of (111) terraces separated by single-atom-height steps of either (100) or (111) orientations, whereas the second class of stepped surfaces consists of (100) terraces and one-atom height of (111) step faces. A compact notation for visualizing the structure of vicinal surfaces was introduced by Lang, Joyner, and Somarjai several years ago.[25] In this notation the surface structure is given in general form $S(h_tk_tl_t)\times(h_sk_sl_s)$, where $(h_tk_tl_t)$ and $(h_sk_sl_s)$ represent the Miller indices of the terrace plane and the step plane, respectively, while S is the number of atoms in the width of terrace, including those in the step and corner chains, as used in Table I. In this paper we have chosen to study Cu(331) and Cu(211), which are vicinals of (111) created by cutting the crystal at an angle of 22° and 19.5° away from the (111) plane toward the [211] and the [211] directions, respectively (see Fig. 1), and Cu(511), which is a vicinal of the (100) surface constructed by slicing the crystal at an angle of 15.8° from the (100) plane toward the [011] direction.

We have taken the *x* and *y* axes to lie in the surface plane, the *x* axis being perpendicular to the step, the *y* axis being along the step, and the *z* axis being along the surface normal, as shown in Fig. 2. As seen from Table I, all three surfaces studied here consist of three chains of atoms and have similar step-step separations. The three chains forming the (111) and (100) terraces are labeled corner chain (CC), terrace chain (TC), and step chain (SC).

Our calculations for the structure of each vicinal surface are performed using a 72-layer supercell which is thick enough so that two surfaces (top and bottom) do not interact. The surface supercell dimensions $N_x\times N_y$, where N_x is the number of terraces and N_y is the number of atoms along the step direction (y), are chosen as 4×6 so as to reduce the size effects along the directions parallel and perpendicular to the step edge. Periodic boundary conditions are applied along the *x* and *y* directions, while no such constraint is imposed along the *z* direction.

III. THEORETICAL METHOD

Since our main interest lies in the projected local vibrational density of states for the SC atoms, a local approach in real space is needed. For this purpose the real-space Green's-function (RSGF) method is used.[26] The essential feature of this method is that it makes no use of the concepts of wave vector and Brillouin zone. In this method one can focus on

TABLE I. Structural notations and features.

Miller index hkl	Compact-step notation $S(h_tk_tl_t)\times(h_sk_sl_s)$	Step edge	Miscut angle (degrees)	Step-step separation (Å)
211	$3(111)\times(100)$	[011]	19.5	6.26
331	$3(111)\times(111)$	[011]	22.0	5.57
511	$3(100)\times(111)$	[011]	15.8	6.64

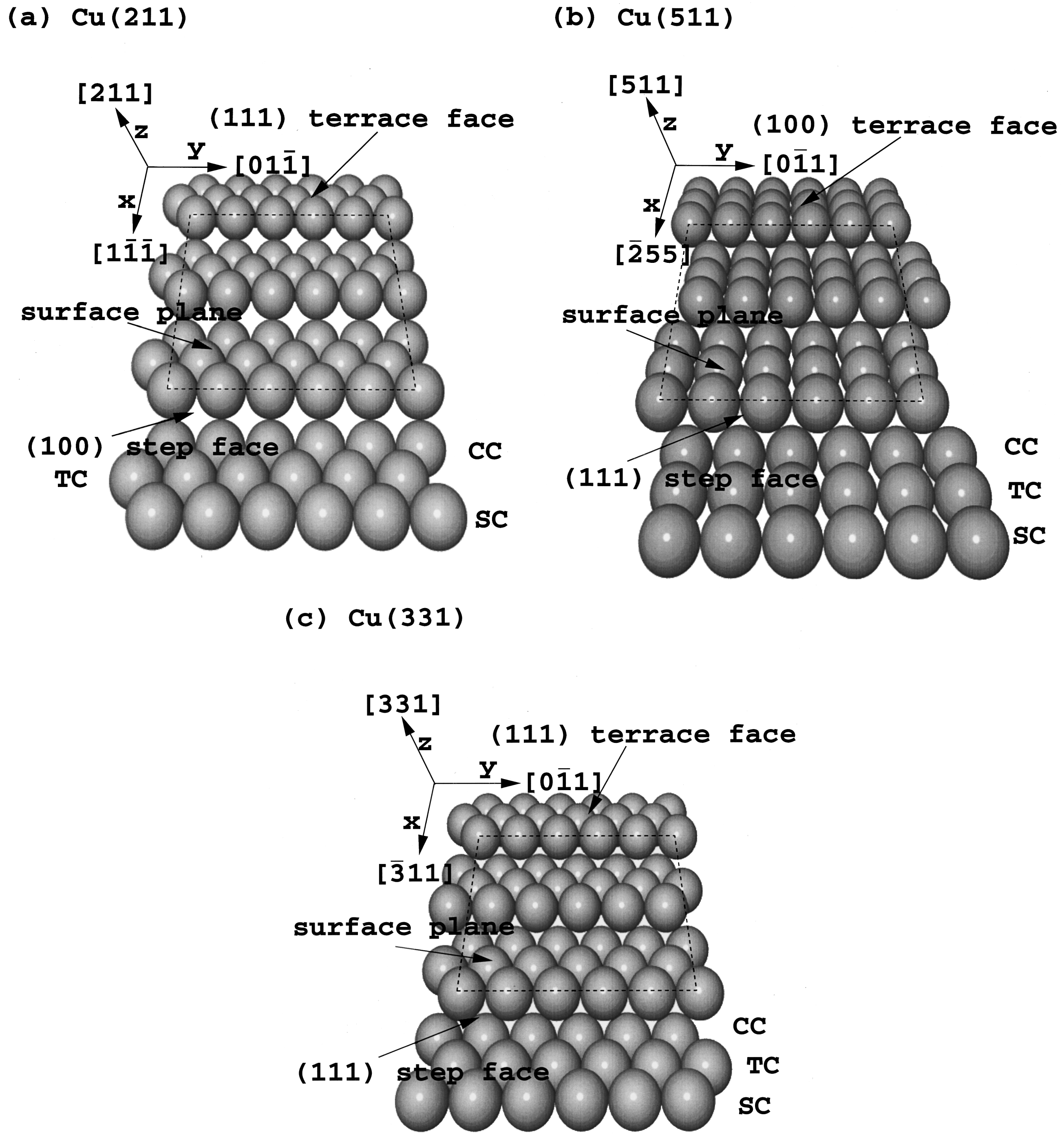

FIG. 2. The (211), (511), and (331) surface geometries.

any local region according to need, and analyze the effect of the rest of the system on that particular region. Also, it does not require the system to be periodic, and thus it is particularly suitable for studying the local vibrational density of states in complex systems with defects, disorder, and reduced symmetry. The only prerequisite to this method is that the interatomic potential between the atoms in the system be of finite range, as it is then possible to write the force-constant matrix in a block-tridiagonal form. Because our purpose is to study surface-atom dynamics, we set up the force-constant matrix in a layer-by-layer manner.[21] Depending upon the range of interatomic potential and the way layers are stacked in the crystal, the number of layers to be included in a locality will be different. Once the force-constant matrix is built in block-tridiagonal form, the Green's-function matrix corresponding to the local region of interest is then constructed following the procedure described in Ref. 26. The normalized vibrational density of states associated with locality i is given by

$$N_i(\omega^2) = -\frac{1}{3n_i\pi}\lim_{\epsilon\to 0}\{\mathrm{Im}[\mathrm{Tr}(G_{ii}(\omega^2+i\epsilon))]\}, \qquad (1)$$

TABLE II. The calculated percentage change in interlayer relaxations $d_{i,i+1}$ and registries $r_{i,i+1}$ for Cu(211), Cu(511), and Cu(331). Here $d_{i,i+1}=100\times[(z_i-z_{i+1})-d_b]/d_b$ and $r_{i,i+1}=100\times[(x_i-x_{i+1})-r_b]/r_b$, where d_b and r_b are the bulk interlayer spacing and registry, respectively.

Surface	d_{12}	d_{23}	d_{34}	d_{45}	d_{56}	d_{67}	d_{78}	d_{89}	d_b
Cu(211)	−10.28%	−5.41%	+7.26%	−5.65%	−1.2%	+3.99%	−2.6%	−0.17%	0.738 Å
Cu(511)	−9.48%	−7.87%	+8.76%	−4.19%	−4.04%	+3.44%	−1.67%	−1.14%	0.696 Å
Cu(331)	−10.42%	+1.72%	−1.66%	−0.27%	−0.3%	+0.54%	−0.37%	+0.15%	0.829 Å

Surface	r_{12}	r_{23}	r_{34}	r_{45}	r_{56}	r_{67}	r_{78}	r_{89}	r_b
Cu(211)	−0.42%	+0.61%	0.00%	0.00%	−0.28%	0.00%	+0.08%	−0.1%	2.087 Å
Cu(511)	−1.86%	−0.39%	+0.80%	−0.24%	−0.41%	+0.54%	0.00%	−0.26%	2.459 Å
Cu(331)	+0.93%	−0.80%	+0.82%	−0.56%	+0.2%	0.00%	0.00%	−0.06%	2.052 Å

with $N_i(w)=2wN_i(w^2)$, where G_{ii} is the Green's-function matrix corresponding to locality i, and n_i is the number of atoms in this locality.

With some effort one can also determine the propagation direction of a surface mode by using the RSGF method. For this purpose, the eigenvector corresponding to a given mode is obtained from the imaginary part of the column vector of the Green's-function matrix associated with the mode. Once the eigenvector (displacement vector) at every site is identified, the wave front of the propagating mode is found by simply linking the sites with identical displacement vectors. The propagation vector is then the vector perpendicular to the wave front. In practice, to obtain the most accurate values for the wave characteristics (polarization and propagation) of a mode at any frequency in the density of states, the width of the Lorentzian (ϵ) needs to be reduced until only one mode is singled out. This is, however, a tedious process and in addition the method itself is not suitable for the calculation of the frequency of a given mode at a specific point in the Brillouin zone, since the density of states contains information from the entire Brillouin zone at each frequency. If one is interested in making a direct link with the experimental data on phonon dispersion, it is better to use a straightforward slab calculation in wave-vector space.[18,19]

To describe the interactions between the atoms in the model systems, we use the embedded-atom method (EAM). This is a semiempirical potential and of many-body type.[27] Although the EAM potentials neglect the large gradient in the charge density near the surface and use atomic charge density for solids for the six fcc metals Ag, Au, Cu, Ni, Pd, and Pt, and their alloys, it seems to have done a quite successful job of reproducing many of the characteristics of the bulk and surface systems.[27] We have also found the EAM potentials to be reliable for examining the temperature dependent structure and dynamics of Cu and Ag flat surfaces,[28] and for describing the energetics of Cu vicinals and self-diffusion processes on the (100) surfaces of Ag, Cu, and Ni.[29,30] Using these interactions for a model system constructed in its bulk-terminated positions, the conjugate-gradient method is used to relax the system to 0-K equilibrium configuration. The dynamical matrix needed for determining the Green's-function matrix is then obtained from analytical expressions for the partial second derivatives of the EAM potentials.[27] As mentioned above, the number of layers to be included in a locality is dictated by the range of interatomic potential and the way layers are stacked in the crystal. The range of EAM potentials for Cu is such that atoms in layer 6 have negligible interactions with those in layer 13. Thus in order to have the force-constant matrix in block-tridiagonal form, at least six layers need to be included in a locality. Since Cu(331) and Cu(211) are vicinals of (111) which has ABC stacking, and Cu(511) is a vicinal of (100) which has AB stacking, in the present study the number of layers in a locality is six for Cu(511) and nine for Cu(331) and Cu(211).

Once the local vibrational density of states is calculated, we can easily determine the local thermodynamic functions of the system which, in the harmonic approximation, are given by

$$F_{\mathrm{vib}}=3k_BT\int_0^\infty \ln\left[2\sinh\left(\frac{\hbar w}{2k_BT}\right)\right]N(w)dw, \tag{2}$$

$$S_{\mathrm{vib}}=3k_BT\int_0^\infty\left[\frac{\hbar w}{2k_BT}\coth\left(\frac{\hbar w}{2k_BT}\right)-\ln\left(2\sinh\frac{\hbar w}{2k_BT}\right)\right]N(w)dw, \tag{3}$$

$$C_v=3k_BT\int_0^\infty\left(\frac{\hbar w}{2k_BT}\right)^2\frac{1}{\sinh^2\left(\dfrac{\hbar w}{2k_BT}\right)}N(w)dw, \tag{4}$$

$$\langle u_\alpha^2\rangle=\frac{\hbar}{2M}\int_0^\infty\frac{1}{w}\coth\left(\frac{\hbar w}{2k_BT}\right)N_\alpha(w)dw, \tag{5}$$

where F_{vib}, S_{vib}, C_v, and $\langle u_\alpha^2\rangle$ are, respectively, the vibrational free energy, the vibrational entropy, the lattice heat capacity, and the mean-square atomic displacements along the Cartesian direction α, and $N(w)$ is the calculated vibrational density of states for the local region of interest.

IV. RESULTS AND DISCUSSIONS

A. Relaxation and force constants near the surface step-chain atom

Due to the loss of neighbors along the z direction for all surface atoms, and along the x direction for the step atoms, the vicinal surfaces relax in both directions, leading to dif-

TABLE III. Percentage change in the bond lengths of the step-chain atom to its nearest neighbors, relative to the bulk nearest-neighbor distance.

Bond	Cu(211)	Cu(511)	Cu(331)
SC-BNN	−2.1%	−2.3%	−3.09%
SC-TC	−1.27%	−2.29%	−0.44%
SC-CC	−2.67%	−0.98%	−1.86%

ferent interlayer separations (z-component relaxation) and interlayer registries (x-component relaxation) at and near the surfaces, as compared to those in the bulk. The calculated percentage interlayer separations and registries for the three stepped surfaces of Cu are presented in Table II. For all surfaces, the largest interlayer relaxations occur for d_{12}. The oscillation of the interlayer relaxations for both the Cu(211) and Cu(511) surfaces is (-,-,+,-,-,+,...) with decreasing magnitude away from the surface into the bulk. It is worth noting that such oscillatory behavior for interlayer relaxations has been reported for Al(511) by Gravil and Holloway[14] and for all fcc(211) surfaces by Jiang, Jona, and Marcus.[15] Results from local-density-approximation calculations and LEED experiment on the surface structure of Al(331) surface reveal a similar oscillatory behavior.[9,11] However, our calculations for the Cu(331) surface show a somewhat different relaxation pattern, i.e., it is (-,+,-,-,-,+, -,+,...). As seen in Table II, the predicted interlayer registry relaxations between the first two layers display contraction for the Cu(211) and Cu(511) surfaces, expansion for Cu(331). The surface structure of Cu(331) thus shows completely different characteristics. We are not aware of any theoretical or experimental study on the surface structure of Cu(331) with which our predictions can be compared.

In Table III, we show the percentage change in the distance of the SC atom to its neighbors, relative to the bulk nearest-neighbor spacing. As seen in Table III, for Cu(331) and Cu(511) the maximum change in the distance appears between the SC atom and the atom just underneath it [bulk nearest neighbor (BNN)]. For Cu(211), however, relaxations cause the largest bond-length change between the SC and CC atoms. The calculated changes in the bond lengths of SC atoms can be understood by analyzing the relaxation in the low coordination region around the step edge. In Fig. 3, we present the relaxation pattern of the atoms on the terrace and of the BNN, for the three vicinal surfaces. The pattern of the SC atoms displays a slight contraction toward the remainder of the metal. An outward relaxation is found for the CC atoms of Cu(511) and Cu(211), and an inward relaxation for the CC atoms of Cu(331). The relaxation of the SC atom is strongly dependent on its surrounding atoms. When it relaxes toward the remainder of the metal in order to maximize its effective coordination, the relaxation should also satisfy the demand of its neighbors, that is the passivization of their lower coordination. As seen in Table IV, the CC atom on Cu(211) has a lower coordination than its counterpart on Cu(331). Clearly, the SC atom on Cu(211) maximizes the effective coordination of both the CC atom and itself, by relaxing toward the CC atom, resulting in the greatest shortening in the bond length between them. For the SC atom on Cu(511), the influence of the lower coordination on the relaxation is even more dramatic. On this surface, the TC atom has a coordination of 8. Evidently, it is this lower coordination of the TC atom that causes the SC atom to relax toward the BNN and TC atom. The fact that the bond-length change between the SC and BNN atoms is almost the same as the one between the SC and TC atoms reflects the influence of the low coordination of the atoms in the local environment of the SC atom (see Table II). On the other hand, it has been reported that, for several vicinal surfaces of Pt(111), the bond lengths of the SC atoms to the BNN are shortened the most.[10] This conclusion supports what we predict for Cu(331). For Pt(331), for example, this particular bond-length change is −4.4%, as compared to −3.09% for Cu(331), in our case. Conversely, our results for Cu(211) are not in agreement with what has been reported for Pt(211). It is also worth noting that although the TC atoms have a different atomic environment from the (111) surface atoms, their relaxation patterns are pretty similar to the latter, as they relax mostly in the direction normal to the terrace. To appreciate the implications of the relaxations of the step at-

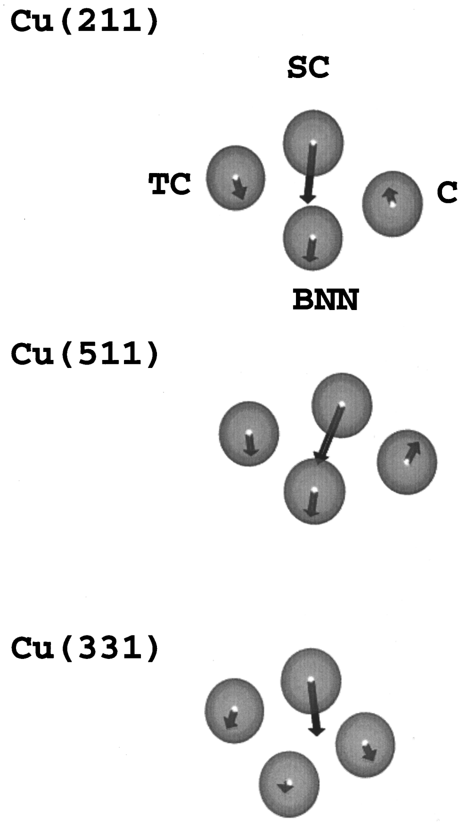

FIG. 3. Relaxation patterns of the atoms at and near the step of Cu(211), Cu(511), and Cu(331). All atomic displacements are magnified.

TABLE IV. The number of neighbors for the surface atoms on the three different stepped surfaces.

Surface	SC	TC	CC
(211)	7	9	10
(511)	7	8	10
(331)	7	9	11

TABLE V. Force-constant matrices $k_{\alpha\beta}$ in (eV/ Å/unit mass) for the interactions between the SC atom on Cu(211) and its nearest neighbors (on the surface and in the bulk).

Atoms		Surface			Bulk		
SC-SC	x	0.0122	0.0613	0.0071	0.0931	0.0000	0.0079
	y	−0.0613	−1.6129	−0.2330	0.0000	−1.9777	0.0000
	z	0.0071	0.2330	0.0008	0.0079	0.0000	0.0987
SC-TC	x	−1.3793	0.8954	−0.6340	−1.2838	0.8500	−0.4907
	y	0.8727	−0.4276	0.3859	0.8500	−0.4204	0.2932
	z	−0.3259	0.2036	−0.1298	−0.4907	0.2932	−0.0818
CC-SC	x	−1.6344	0.0000	1.0355	−1.2837	0.0000	0.9814
	y	0.0000	0.0898	0.0000	0.0000	0.0875	0.0000
	z	1.3683	0.0000	−0.7534	0.9814	0.0000	−0.5897
BNN-SC	x	0.1237	0.0162	−0.0582	0.0931	−0.0069	−0.0040
	y	−0.0140	−0.5070	1.1120	−0.0069	−0.4204	0.8991
	z	−0.0770	1.9530	−1.9071	−0.0040	0.8991	−1.4587

oms on the three stepped surfaces of Cu, we now turn to an examination of the force-constant matrices associated with them.

In Tables V, VI, and VII, we present the force-constant matrices $k_{\alpha\beta}$, where α and β stand for Cartesian components, as obtained from EAM potentials between the SC atoms and their neighbors on the Cu(211), Cu(511), and Cu(331) surfaces, respectively. The force constants k_{xx} between the SC atoms in the direction perpendicular to the step, in the surface plane, are softened 86% for Cu(211), 93% for Cu(511), and 85% for Cu(331), relative to their counterparts in the bulk, due to the loss of neighbors. This unpreventable softening causes the density of states for the step atom along the x direction to be shifted strongly to lower frequencies. Such a softening in the force constant between SC atoms has also been reported for Ni(977) (Refs. 17 and 24) and for Au(511).[22] The k_{zz} element between SC and BNN atoms on Cu(211), Cu(511), and Cu(331) are, respectively, stiffened by 30%, 35%, and 45%. The stiffening of this force constant on Cu(331) and Cu(511) is obviously the reason for the strong contraction in their bond lengths. From the tables we also notice that the existence of steps on the surface induces changes not only on the diagonal elements of the force-constant matrices of the surface atoms, but also on the off-diagonal elements. For example, k_{xz} and k_{yz} between SC and BNN atoms on Cu(511) are stiffened by 30% and 35%, respectively.

B. Local vibrational density of states for the step-chain atoms

In Fig. 4 we present the calculated local vibrational density of states for the SC atoms on the (211), (511), and (331) surfaces of Cu along the x, y, and z directions. Note that there is a marked richness in these density of states (SC-

TABLE VI. Force-constant matrices $k_{\alpha\beta}$ in (eV/Å/unit mass) for the interactions between the SC atom on Cu(511) and its nearest neighbors (on the surface and in the bulk).

Atoms		Surface			Bulk		
SC-SC	x	0.0057	0.0167	−0.0050	0.0887	0.0000	−0.0044
	y	−0.0167	−1.6104	−0.2388	0.0000	1.9777	0.0000
	z	−0.0050	0.2388	0.0380	−0.0040	0.0000	0.1030
SC-TC	x	−2.1859	0.0000	−0.8307	−1.8234	0.0000	−0.5452
	y	0.0000	0.0678	0.0000	0.0000	0.0875	0.0000
	z	−0.3896	0.0000	−0.1067	−0.5452	0.0000	−0.0499
CC-SC	x	−0.9416	−0.7116	0.6304	−0.8418	−0.7037	0.7594
	y	−0.7637	−0.4282	0.4892	−0.7037	−0.4205	0.5598
	z	0.8832	0.6337	−0.5432	−0.7594	0.5598	−0.5238
BNN-SC	x	−0.0683	0.3926	−0.5996	−0.0769	0.3062	−0.4846
	y	0.3822	−0.5201	1.0726	0.3062	−0.4205	0.8454
	z	0.6337	1.1648	−1.7441	−0.4846	0.8454	−1.2888

TABLE VII. Force-constant matrices $k_{\alpha\beta}$ in (eV/Å/unit mass) for the interactions between the SC atom on Cu(331) and its nearest neighbors (on the surface and in the bulk).

Atoms		Surface			Bulk		
SC-SC	x	0.0149	0.0456	-0.0008	0.1034	0.0000	-0.0038
	y	-0.0456	-1.6045	-0.2369	0.0000	-1.9777	0.0000
	z	-0.0008	0.2369	-0.0055	-0.0038	0.0000	0.0883
SC-TC	x	-1.2389	-0.7979	-0.6305	-1.2436	-0.8310	-0.5361
	y	-0.7815	-0.3905	0.3957	-0.8310	-0.4204	-0.3432
	z	-0.3288	-0.2154	-0.1622	-0.5361	-0.3432	-0.1220
CC-SC	x	-0.6906	0.6684	0.7882	-0.5914	0.5903	0.7704
	y	0.7191	-0.4868	-0.7498	0.5903	-0.4204	-0.6782
	z	-0.9997	-0.8795	-0.9733	0.7704	-0.6782	-0.7741
BNN-SC	x	-0.0153	0.0456	-0.7127	-0.0053	0.0000	-0.4649
	y	0.0000	0.1392	0.0000	0.0000	0.0875	0.0000
	z	-0.7140	0.0000	-2.7106	-0.4649	0.0000	-1.8681

DOS) compared to the smoother DOS for the bulklike atom, indicating a different nature of the bonding between atoms on vicinal surfaces from those in the bulk. Also, the low-frequency modes of step atoms on all vicinal surfaces are shifted overall toward lower frequencies as compared to the corresponding bulk modes (dark solid line), in all directions. The most softening appears along the x direction, which may be traced to the loss of neighbors for the SC atoms. Although (511) and (211) are vicinals of different low Miller-index surfaces, the SC atoms on these surfaces have similar atomic environments, as they both have one face of (100) [step face of (211) and terrace face of (511)] and another face of (111) [terrace face of (211) and step face of (511)]. In contrast, the SC atoms on the (331) surface have two faces of the same (111) orientation (step and terrace faces). The fact that the densities of states for the SC atoms on the (511) and (211) surfaces are similar, and that of the DOS for the (331) surface is different, seems to echo the effect of the atomic environment on the local density of states.

As seen in Fig. 4, for the Cu(211) surface, the most distinguished low-frequency mode appears at 2.524 THz with vibrations most pronounced along the x direction. All terrace atoms participate in this mode, with the displacement pattern shown in Fig. 5(a). Note that while the SC and CC atoms move alternately in the $+x$ and $-x$ directions with a z component, the TC atoms vibrate along the y direction with no x and z components. The displacement vectors associated with their motion are presented in Table VIII. From the displacement vectors for the SC atoms, it is clear that this low-frequency mode corresponds to the wave propagating along the step (along y) with a wavelength $\lambda=2\times$(nearest-neighbor distance$=5.11$ Å) and a wave vector $k=(0.0,1.229\ \text{Å}^{-1},0.0)$, i.e., it is a mode at the zone boundary associated with the direction along the step edge. We have also reported a very similar mode for the Ni(977) surface at 3.3 THz.[24] Remember that the (977) is an A-type vicinal of the (111) surface, like the (211) surface, with eight $\langle 0\overline{11}\rangle$ chains on the terrace. The displacement patterns of the TC, SC, and CC atoms on the Ni(977) surface are pretty similar to what we present here for the surface atoms on Cu(211). The mode on Ni(977) is a *super*localized mode since it involves only the concerted motion of the SC and CC atoms in conjunction with the TC atoms next to the step edge. It is interesting that, with increasing terrace width, this low-frequency mode becomes a *super*localized mode. This calculated mode with a frequency 2.524 THz [for Cu(211)] is in excellent agreement with the He-atom scattering measurements by Witte *et al.*,[18] who found a horizontal low-frequency mode (T) at 2.684±0.2 THz. These authors also performed a lattice-dynamical slab calculation using only a single radial force constant for the nearest-neighbor interactions, to determine the displacement patterns and polarizations of the observed modes. The displacement patterns they reported for the surface atoms are quite similar to what we find here. However, our calculations for BNN atoms yield displacement patterns which are different from the ones found by Witte *et al.*. In our case atoms vibrate along the y

TABLE VIII. Displacement vectors (x,y,z) of the surface atoms of Cu(331), Cu(211), and Cu(511) for low-frequency modes. All displacement amplitudes are normalized.

Atom	Cu(331) $f=2.916$ THz	Cu(211) $f=2.524$ THz	Cu(511) $f=2.247$ THz
CC	$(-0.3492, 0.0000, -0.2695)$	$(-0.5245, 0.0000, 0.7258)$	$(0.5271, 0.0000, 0.4788)$
TC	$(0.0000, -0.3325, 0.0000)$	$(0.0000, -0.2009, 0.0000)$	$(0.8972, 0.0000, 0.2885)$
SC	$(1.0000, 0.0000, 0.3429)$	$(1.0000, 0.0000, -0.2975)$	$(1.0000, 0.0000, -0.0687)$

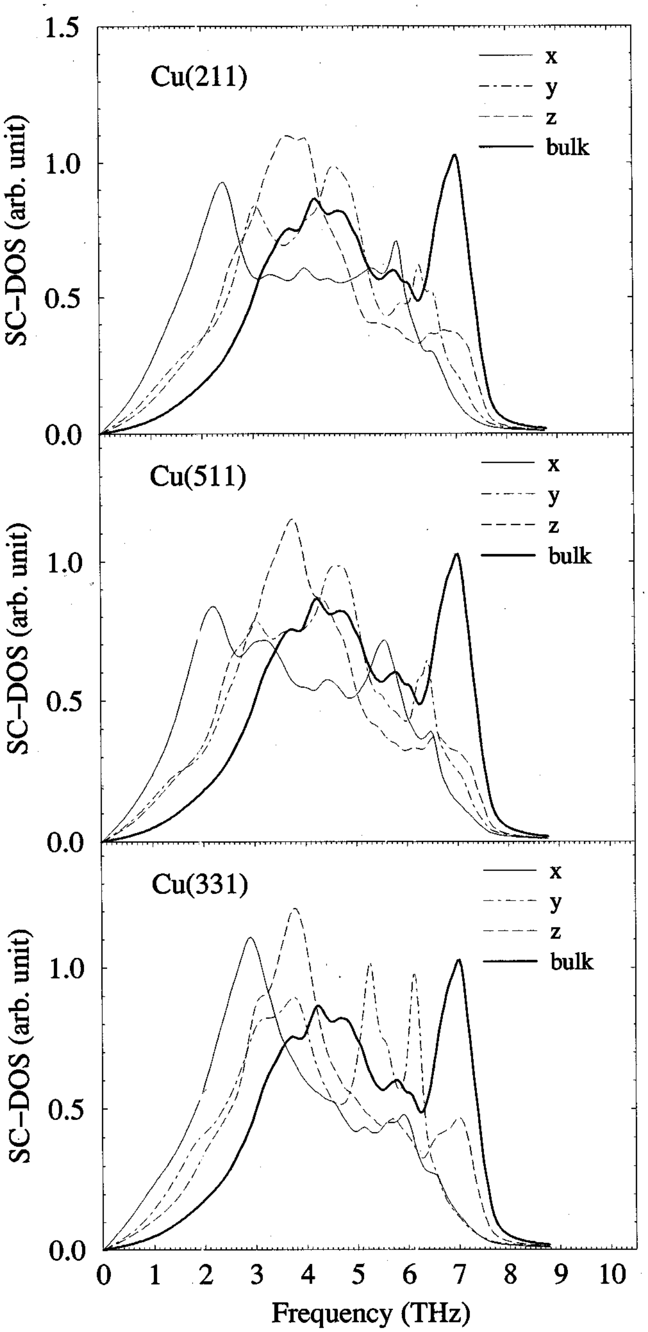

FIG. 4. Vibrational density of states for the step atoms (SC-DOS) of Cu(211), Cu(511), and Cu(331), together with the bulk DOS.

direction with no x and z components. As pointed out in Ref. 18, the simple one-force-constant model is not sufficient to explain all characteristics of surface phonons on stepped surfaces. An additional low-frequency shear horizontal mode in which all chains on the terrace move alternately along the $+y$ and $-y$ directions is found at 3.095 THz. The wavelength of this mode is (2×one terrace length=12.518 Å), and its wave vector k=(0.0, 0.5 Å^{-1}, 0.0). It is thus a zone-boundary mode with a propagation perpendicular to the step edge. The displacement patterns of the surface atoms are shown in Fig. 5(b).

For Cu(331), a low-frequency mode propagating along the step is found at 2.916 THz. The density of states for the SC atoms on Cu(511) reveals a similar low-frequency mode with a polarization mostly in the x direction at 2.247 THz. These low-frequency modes on Cu(331) and Cu(511) have the same wave characteristics (wavelength, wave vector, propagation direction) as the low-frequency mode on Cu(211). The displacement vectors of the terrace atoms on the surface are included in Table VIII. However, there is a pictorial difference between displacement patterns of surface atoms on Cu(211), Cu(331), and Cu(511). The terrace atoms on Cu(331) and Cu(211) have similar displacement patterns, whereas those on Cu(511) are different. The TC atoms on vicinals of the (111) surface move backward and forward along the y direction. In contrast, the TC atoms on Cu(511), which is a vicinal of (100), vibrate mostly perpendicularly to the step edge, as do the other atoms on the terrace. These results indicate that when a chain of atoms starts vibrating with a component perpendicular to the chain, in the terrace plane, the atoms of the next chain, on vicinals of (111), vibrate along the chain, whereas those on vicinals of (100) follow the motion of the first chain (see Figs. 5 and 6). For Cu(331), besides the low-frequency mode, the density of states reveals two higher-frequency modes with dominant vibrations along the y direction at 5.256 and at 6.119 THz (inside the bulk band).

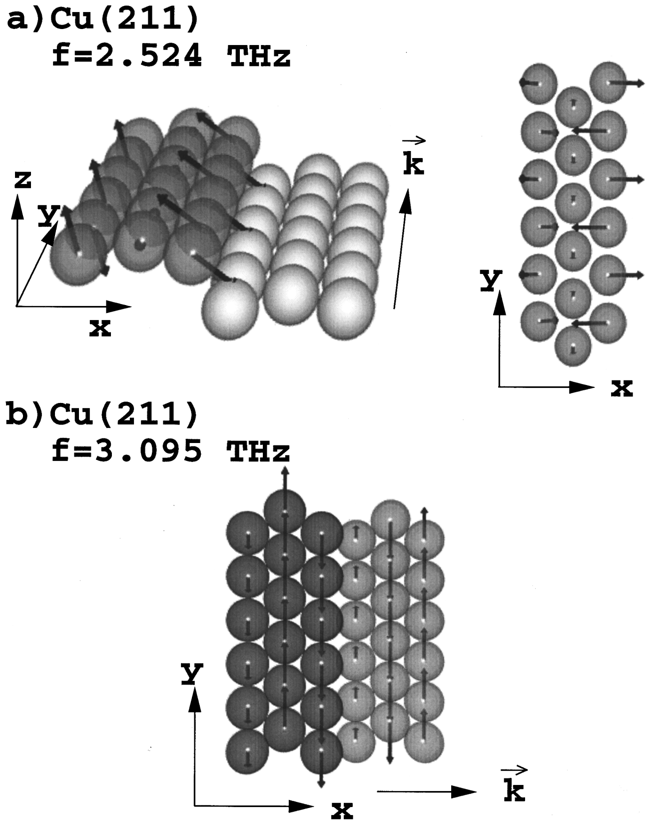

FIG. 5. Displacement patterns of the Cu(211) surface atoms for the low-frequency phonon modes with the propagation (a) along and (b) perpendicular to the step edge.

C. Local thermodynamic properties of the SC atoms

With the calculated local vibrational density of states of the SC atoms at hand, we have also determined the local

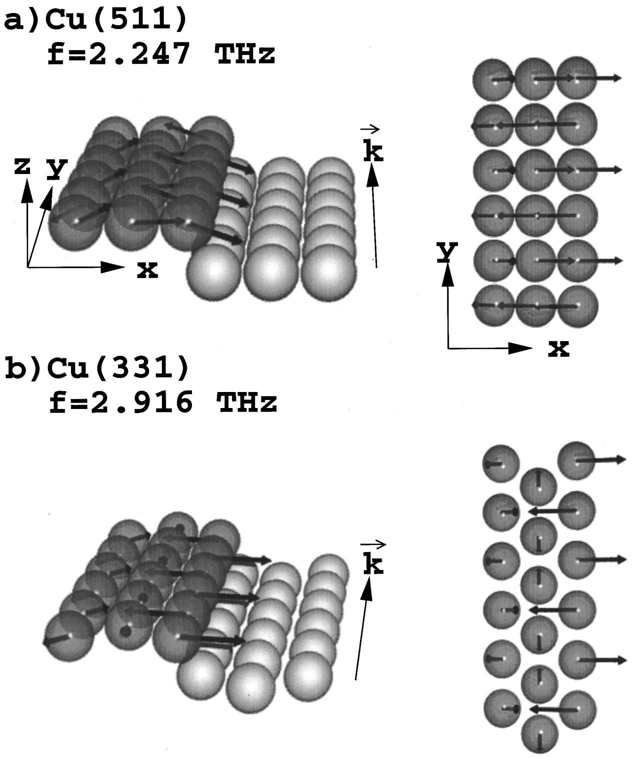

FIG. 6. Displacement patterns of the surface atoms on (a) Cu(511) and (b) Cu(331) for the low-frequency phonon modes along the y direction. On the right, the top view of the displacement patterns is shown.

thermodynamic functions of the SC atoms using Eqs. (2)–(5). We find that the thermodynamic functions for the SC atoms on the three different surfaces are almost the same, revealing the sensitivity of the local thermodynamic functions to the local atomic coordination. The thermodynamic functions for the step-chain atom on the Cu(211) surface are shown in Fig. 7.

In Fig. 8, the calculated mean-square vibrational amplitudes for the SC, TC, and CC atoms on the Cu(211) surface are plotted. In this plot, the x, y, and z directions are, respectively, along the terrace, along the step edge, and normal to the terrace. Note that the most dominant displacement of a step atom is along the x direction, in which the SC atom has the most room to move. Here we observe that the largest value of the mean-square vibrational amplitude along the x direction appears for the SC atoms, followed by that for the TC atoms, and then that for the CC atoms, reflecting the order in the coordination number (7, 9, and 10, respectively), while the order is the reverse for displacements along the z direction. In contrast, the displacements along the step edge (y) are more or less the same for all three vicinals at low temperatures ($T<50$ K), and that of SC atoms increase a bit more rapidly than that of TC and CC atoms at higher temperature. At these temperatures, however, anharmonic effects should become important and need to be included in the calculations.

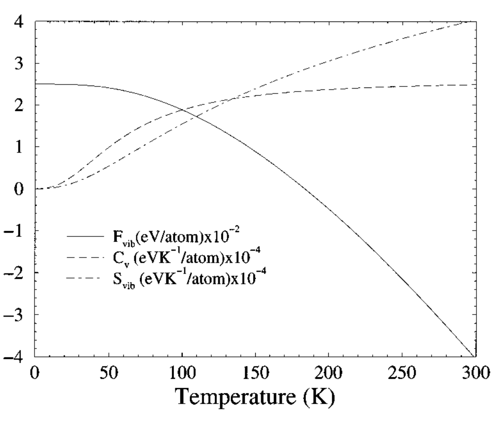

FIG. 7. The local thermodynamic functions: vibrational free energy (F_{vib}), lattice heat capacity (C_v), and vibrational entropy (S_{vib}) for the SC atoms on Cu(211).

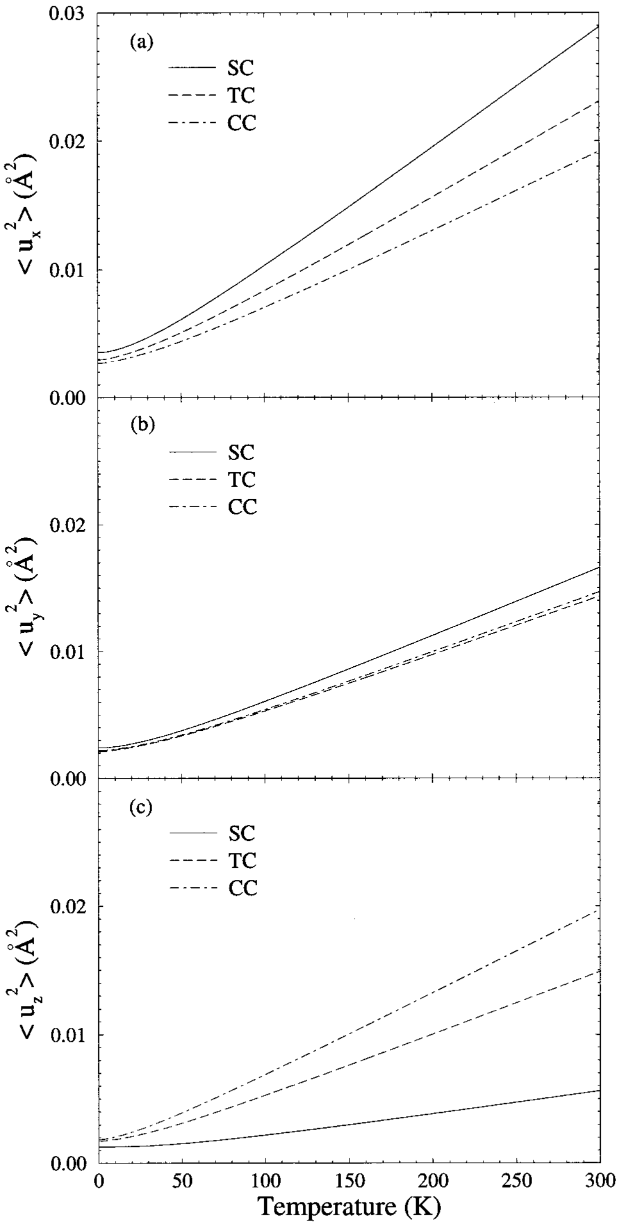

FIG. 8. Calculated mean-square displacements for the SC, TC, and CC atoms on Cu(211) along (a) x, (b) y, and (c) z directions.

In summary, we have explored the local structural and vibrational properties of the SC atoms of three different types of vicinal surfaces of Cu, employing the embedded-atom method for the interaction potentials and the real-space Green's-function technique for the evaluation of the phonon density of states. From an investigation of multilayer relaxations of these surfaces, it is seen that Cu(331) has completely different characteristics from Cu(211) and Cu(511), which exhibit similar characteristics. For all three surfaces, relaxations induce about 30–45 % stiffening in the force constant between SC atoms and their bulk nearest neighbors in the direction normal to the surface plane, yielding a strong contraction in their bond length. For Cu(331) and Cu(511), the bond length of the step atom to its bulk nearest neighbor is shortened the most, whereas for Cu(211) the contraction in the bond length between the SC and CC atoms is the most. We find that the frequencies of the vibrational modes are softened the most for the step atoms along the direction perpendicular to the step edge in the surface plane, resulting from the large reduction in the force constants (85–93 %) between two SC atoms in the same direction. Moreover, the vibrational properties and the relaxations of the step atoms are found to be sensitive to their local atomic environment. The local vibrational density of states, and hence the ensuing thermodynamic properties, for Cu(211) and Cu(511) are found to be almost identical, and point to the similarity of their local atomic environment. While these studies have provided insight into the force-constant changes at and near steps and their relationship to surface relaxations and the appearance of localized modes, they have also increased our need to understand the microscopic changes in the electron charge densities at these steps and the nature of the bonding between atoms. Future work using *ab initio* electronic calculations on the types of surfaces discussed here will be very useful in putting the conclusions drawn presently on a firmer footing.

ACKNOWLEDGMENTS

We thank Pavlin Staikov for delightful discussions. One of us, S.D., acknowledges financial support from the Ministry of Education of Turkey. This work was supported in part by the KSTAR/NSF-EPSCoR program under Grant No. 006169. Computations were carried out on the Convex Exampler SMP funded by Grant No. DMR-9413513 from the National Science Foundation.

---

[1] For a revew, see K. Wandelt, Surf. Sci. **251/252**, 387 (1991).

[2] For a review, see E. D. Williams, Surf. Sci. **299/300**, 502 (1994).

[3] R. Smoluchowsky, Phys. Rev. **60**, 661 (1941).

[4] H. Ibach and D. Bruchmann, Phys. Rev. Lett. **41**, 958 (1978).

[5] G. Allan, Surf. Sci. **85**, 37 (1979).

[6] G. Armand and P. Masri, Surf. Sci. **130**, 89 (1983).

[7] J. E. Black and P. Bopp, Surf. Sci. **140**, 275 (1984).

[8] M. Wuttig, C. Oshima, T. Aizawa, R. Souda, S. Otani, and Y. Ishizawa, Surf. Sci. **193**, 180 (1987).

[9] J. S. Nelson and P. J. Feibelman, Phys. Rev. Lett. **68**, 2188 (1992).

[10] P. J. Feibelman, Phys. Rev. B **52**, 16845 (1995).

[11] D. L. Adams and C. S. Sorensen, Surf. Sci. **166**, 495 (1986).

[12] B. Visscher, A. L. Boers, L. K. Verheij, and B. Poelsema, Appl. Surf. Sci. **26**, 121 (1986).

[13] R. N. Barnett, U. Landmann, and C. L. Clevland, Phys. Rev. Lett. **51**, 1359 (1983).

[14] P. A. Gravil and S. Holloway, Phys. Rev. B **53**, 11 128 (1996).

[15] P. Jiang, F. Jona, and P. M. Marcus, Phys. Rev. B **35**, 7952 (1987).

[16] A. Lock, J. P. Toennies, and G. Witte, J. Electron. Spectros. **54/55**, 309 (1990).

[17] L. Niu, D. D. Koleske, D. J. Gaspar, and S. J. Sibener, J. Chem. Phys. **102**, 9077 (1995).

[18] G. Witte, J. Braun, A. Lock, and J. P. Toennies, Phys. Rev. B **52**, 2165 (1995).

[19] P. Knipp, Phys. Rev. B **40**, 7993 (1989); **43**, 6908 (1991).

[20] Z. J. Tian and J. E. Black, Surf. Sci. **303**, 395 (1994).

[21] A. Kara, C. S. Jayanthi, S. Y. Wu, and F. Ercolessi, Phys. Rev. Lett. **72**, 2223 (1994).

[22] A. Kara, C. S. Jayanthi, S. Y. Wu, and F. Ercolessi, Phys. Rev. B **51**, 17 046 (1995).

[23] A. Kara, S. Durukano$\widetilde{\text{g}}$lu, and T. S. Rahman, Phys. Rev. B **53**, 15 489 (1996).

[24] A. Kara, S. Durukano$\widetilde{\text{g}}$lu, and T. S. Rahman, J. Chem. Phys. **106**. 2031 (1997).

[25] B. Lang, R. W. Joyner, and G. A. Somorjai, Surf. Sci. **30**, 454 (1972).

[26] S. Y. Wu, J. Cocks, and C. S. Jayanthi, Phys. Rev. B **49**, 7957 (1994).

[27] S. M. Foiles, M. I. Baskes, and M. S. Daw, Phys. Rev. B **33**, 7983 (1986); M. S. Daw, S. M. Foiles, and M. I. Baskes, Mater. Sci. Rep. **9**, 251 (1993).

[28] L. Yang and T. S. Rahman, Phys. Rev. Lett. **67**, 2327 (1991); L. Yang, T. S. Rahman, and M. B. Daw, Phys. Rev. B **44**, 13 725 (1991); T. S. Rahman, in *Condensed Matter Theory*, edited by J. W. Clark, K. A. Shoaib, and A. Sadiq (Nova, New York, 1994),Vol. 9, p. 299.

[29] Z. J. Tian and T. S. Rahman, Phys. Rev. B **47**, 9751 (1993).

[30] U. Kuerpick and T. S. Rahman, in *Surface Diffusion: Atomistic and Collective Processes*, edited by M. C. Tringides (Plenum, New York, in press).